IOP Conf. Series: Materials Science and Engineering **1302** (2024) 012002 doi:10.1088/1757-899X/1302/1/012002

Strength and Fracture Toughness of Type 304 and 316 Austenitic Stainless Steels at 4.2 K

Takeru Sakurai[1], Osamu Umezawa[2], Yoshinori Ono[3]

[1]National Institutes for Quantum Science and Technology, Naka, Ibaraki 311-0193, Japan
[2]Yokohama National University, Hodogaya, Yokohama, 240-8501, Japan
[3]National Institute for Materials Science, Tsukuba, Ibaraki 305-0047, Japan

Email: sakurai.takeru@qst.go.jp

Abstract. The tensile properties and fracture toughness of type 304L, 316L and 316LN austenitic stainless steels and their weldments at cryogenic temperatures have been summarized in the literature. Rolled plates showed a trade-off relationship between 0.2% proof stress and plane-strain fracture toughness with those at 4.2 K. The 0.2% proof stress increases with increasing *C+N* content, and the fracture toughness depends on their austenite stability to α'-martensitic transformation at the crack tip. The formation of shear bands at low strains is directly related to fracture toughness. The stacking fault energy represents the shear-band formation as well as slip deformation manner, so alloy design with higher Ni, Mn, and Mo contents in the chemical composition range of 316LN would be desirable to improve fracture toughness due to higher stacking fault energy.

1. Introduction

The austenitic stainless steels, such as type 304L (18Cr-9Ni, in mass%) and 316L (16Cr-10Ni-2Mo), have been widely used in cryogenic applications, especially below 20 K. However, their strength is not sufficient for superconducting applications, such as magnets for fusion reactors and accelerators. Therefore, type 316LN (17Cr-11Ni-2Mo-0.2N) nitrogen-strengthened austenitic stainless steel is commonly used due to its high strength and toughness, and excellent weldability [1]. In addition, increasing the nitrogen content improves austenite phase stability to α'-martensitic transformation and corrosion resistance [2,3]. The 0.2% proof stress at 4.2 K is generally proportional to the nitrogen (plus carbon) content in the composition range of 316LN, and thick plates with 0.2% proof stresses of 1000 MPa or higher have been produced [4]. Thus, type 316LN steel provides an excellent balance of mechanical properties such as strength and toughness, corrosion resistance, and weldability, making it a key structural material for cryogenic applications.

However, as shown by the NIST trend line [5], there is a trade-off relationship where an increase in 0.2% proof stress results in a decrease in fracture toughness. This relationship also applies to welds. Since most superconducting devices are fabricated by welding materials together, it is important to understand the weldability and mechanical properties of welded joints. This reference (NIST trend line, JAERI box [6,7] as a development target) can serve as a useful decision-making tool during initial mechanical design as well as for further alloy development. In recent years, the more ideal type 316LN steel has been developed using these references. This report summarizes the previously reported data for type 304L, 316L, 316LN and their weldments, focusing on tensile properties and fracture toughness, including the trade-off relationship, and presents the development policy for new cryogenic materials.

2. Materials and Test Procedures

The reference data in this report are those reported for type 304L [8-13], 316L [8,9,14,15], and 316LN [13,15-26] base materials and for weldments using type 304L [9,16,27-30], 316L [9,16,27-29,31], and 316LN [16,32,33] base materials for tensile properties, fracture toughness, or both at cryogenic temperatures. The base materials have a low carbon content (approximately 0.05 mass%) to suppress intergranular precipitation of chromium carbides and to ensure strength and toughness at low temperatures. The base materials are melted to a specified chemical composition, hot rolled or forged, solution heat treated at approximately 1323 K, and water quenched. Welding methods include gas tungsten arc welding (GTAW), which does not melt the electrode; shielded metal arc (SMA) welding, submerged arc welding (SAW), metal inert gas (MIG), and metal active gas (MAG), which melt the electrode; and laser beam welding (LBW) and electron beam welding (EBW), which use a high-power beam. The electrode or filler metal is similar in composition to the base materials, such as E316, 316, 308 and 304.

Tensile test data were obtained by immersion in liquid helium (4.2 K), liquid hydrogen (20 K), and liquid nitrogen (77 K), as well as data obtained in the ambient air (approximately 300 K). Fracture toughness tests were also performed by immersion in liquid helium. The fracture toughness evaluation method confirms to ASTM E1820. *J*-integral values are converted to plane-strain fracture toughness values as $K_{IC}(J)$. For a rigorous comparison, parameters such as material manufacturing and test methods should be standardized, but in the interest of summarizing current data, some variation in these parameters is included.

Hot cracking is a problem in the welding of austenitic stainless steels [34]. Suutala and DeLong's diagrams have been used to evaluate weldability [34,35]. The Suutala diagram predicts the weld susceptibility to solidification cracking by plotting the *Ni* and *Cr* equivalents (*Ni* eq. and *Cr* eq.) calculated from the chemical composition for the 304L, 316L, 316LN steels and their weldments as shown in figure 1. The plots of 316LN base materials were labeled as from "a" to "w", because some of them showed a good balance of high strength and high toughness. Most of the data is in the zone where solidification cracking is unlikely to occur. Low levels of impurities such as phosphorus, *P*, and sulfur, *S*, would be favorable. On the other hand, the DeLong's diagram can predict the ferrite content (%) or ferrite number (FN) by plotting the *Ni* eq. and *Cr* eq. as shown in figure 2 [34]. Many of the plots for the 316LN base materials are 0 ferrite due to the stable austenitic phase. Particularly in the case of weldments, it can be seen that the data is distributed from 0 FN to approximately 12 FN. In general, a ferrite content of about 5 to 10% is effective for a good weld, so these data generally indicate good weldability.

3. Data Analysis

For tensile properties and fracture toughness, the results are summarized in terms of temperature dependence at first. Then, the results are presented in terms of *C*+*N* content, which affects strength. Finally, the relationship between 0.2% proof stress and fracture toughness is discussed.

Figure 3 shows the tensile properties (0.2% proof stress: $\sigma_{0.2}$, ultimate tensile strength: σ_B, elongation: EL, reduction of area: RA) plotted against the test temperature on the horizontal axis. For the base material 316LN, the increase in $\sigma_{0.2}$ is more significant at lower temperatures, whereas for the $\sigma_{0.2}$ of the 304L, it tends to remain almost the same level at different temperatures, indicating that the solid solution strengthening by nitrogen has a significant effect on the $\sigma_{0.2}$. σ_B also increases at lower temperatures, but there is little difference between the steel types (304L, 316L and 316LN). $\sigma_{0.2}$ and σ_B trends were generally similar for both base materials and weldments. Although EL and RA tend to decrease at lower temperatures, the RA of weldment at 20 K is lower than that at 4.2 K, as shown in figure 3(h). This may be due to a higher susceptibility to hydrogen embrittlement in ferrite-containing weldments. EL and RA are generally lower for weldments than for base materials due to the hardening of the material caused by the heat input during welding. Weldments have a greater variation, even for the same type. It has been suggested that EL and RA are influenced by the slight difference in the chemical composition of the weld metal, welding method and welding conditions.

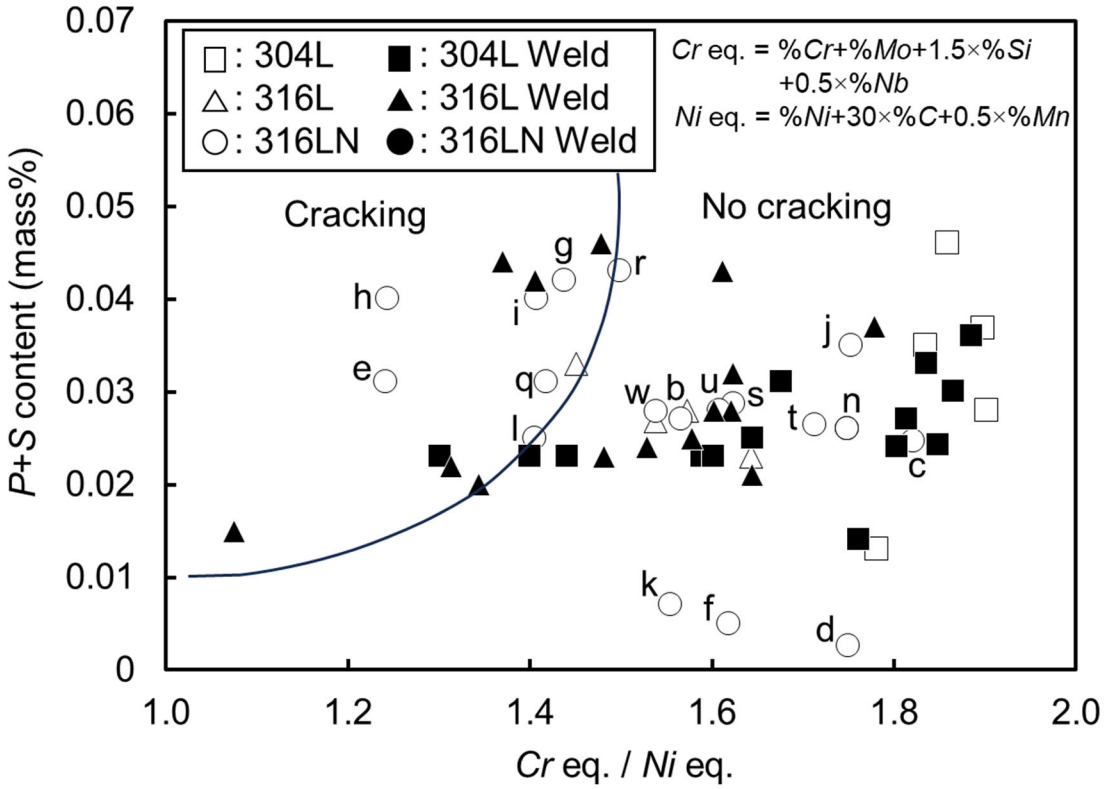

Figure 1. Suutala diagram showing the data of type 304L, 316L, and 316LN steels and their weldments. Each plot of Type 316LN is labeled as a [13], b [15], c [16], d-l [17], m [18], n [19] o [20], p [21], q,r [22], s [23], t,u [24], v [25], and w [26], respectively.

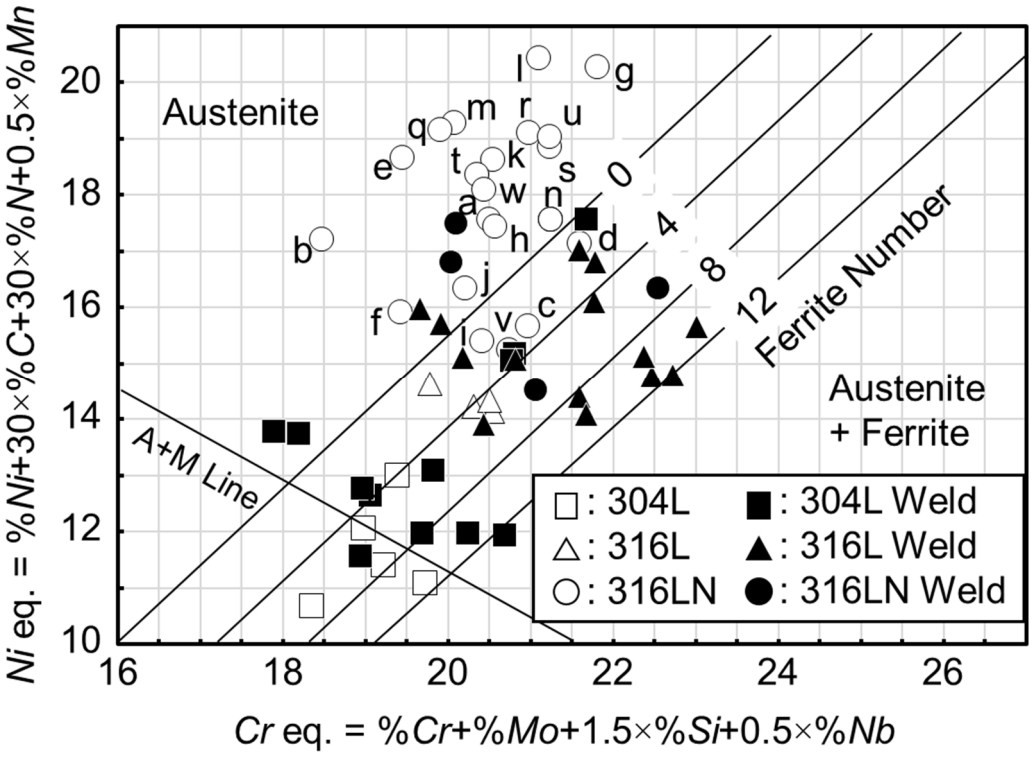

Figure 2. DeLong's diagram plotting data of type 304L, 316L, and 316LN steels and their weldments.

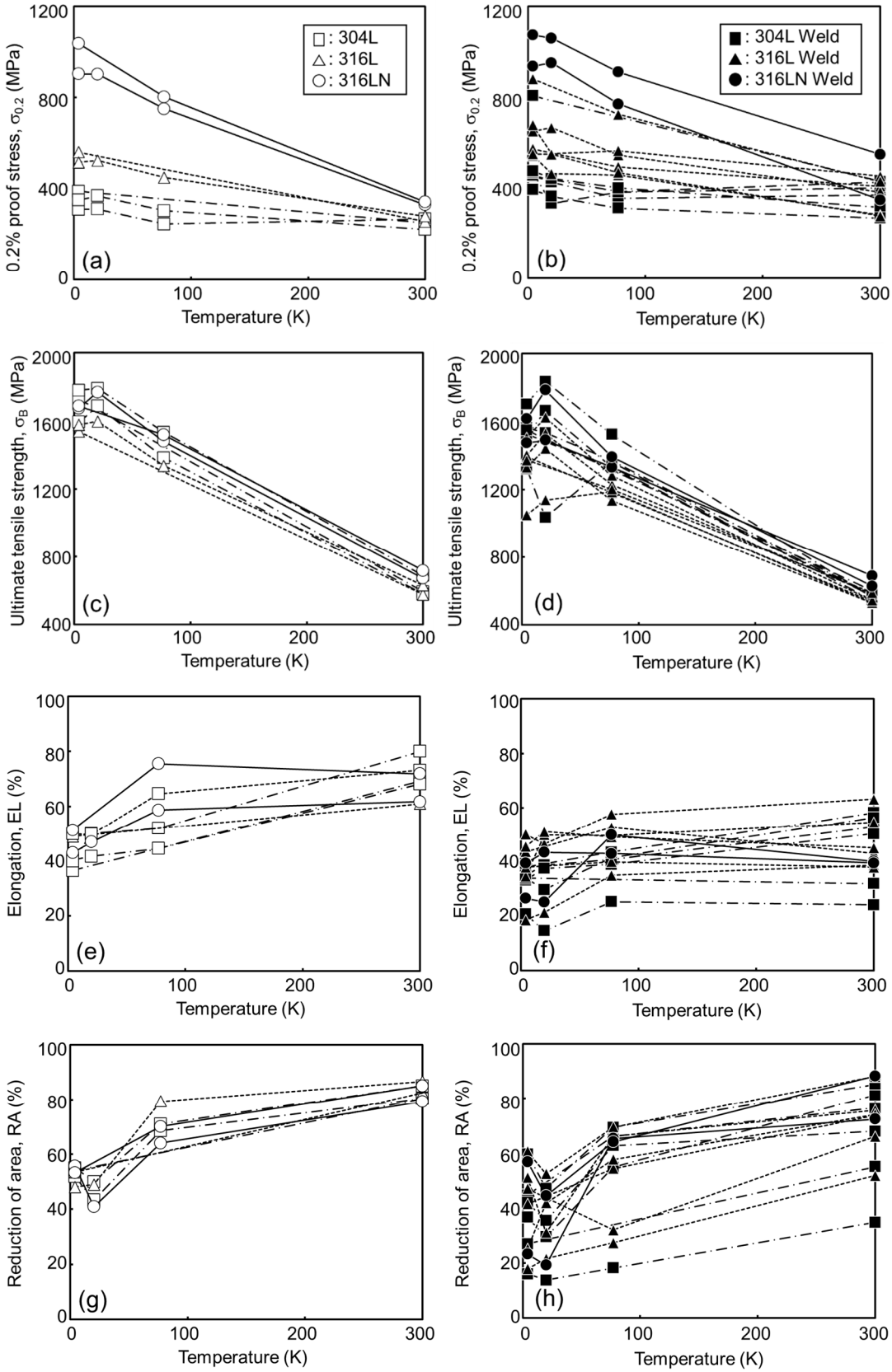

Figure 3. Tensile properties of type 304L, 316L, and 316LN steels and their weldment at cryogenic temperatures: (a), (b) 0.2% proof stress, $\sigma_{0.2}$, (c), (d) ultimate tensile strength, σ_B, (e), (f) elongation, EL, and (g), (h) reduction of area, RA.

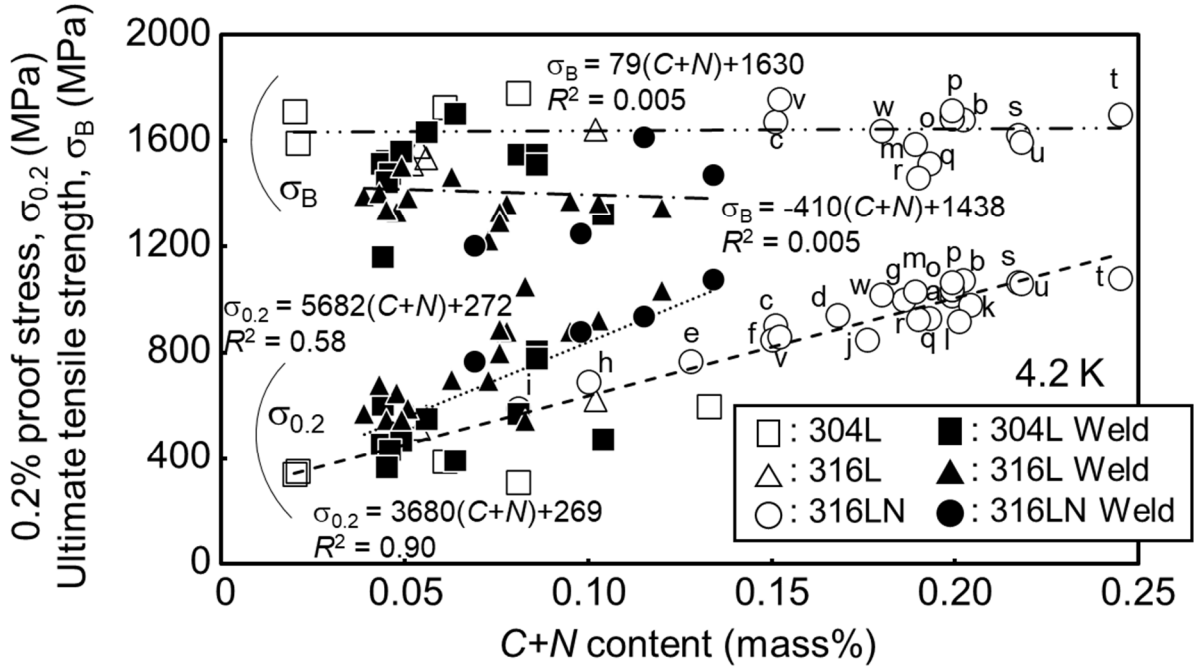

Figure 4. Relationship between *C+N* content and strength ($\sigma_{0.2}$ and σ_B) at 4.2 K for type 304L, 316L, and 316LN steels and their weldments.

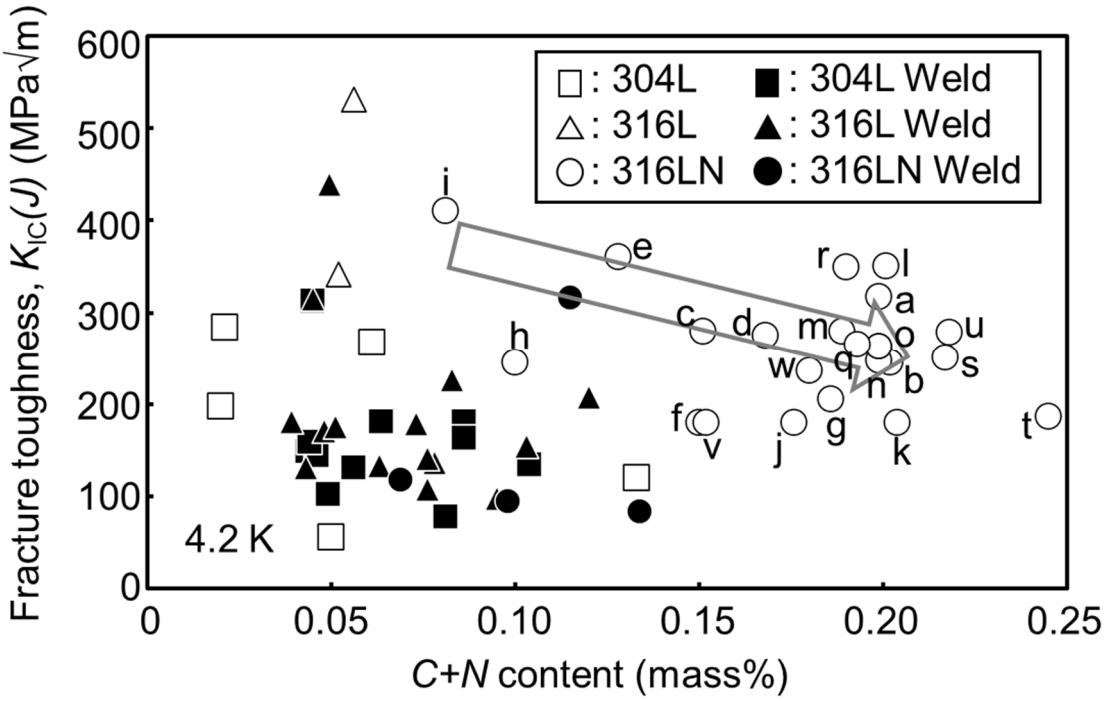

Figure 5. Relationship between *C+N* content and fracture toughness, $K_{IC}(J)$, at 4.2 K for type 304L, 316L, and 316LN steels and their weldments.

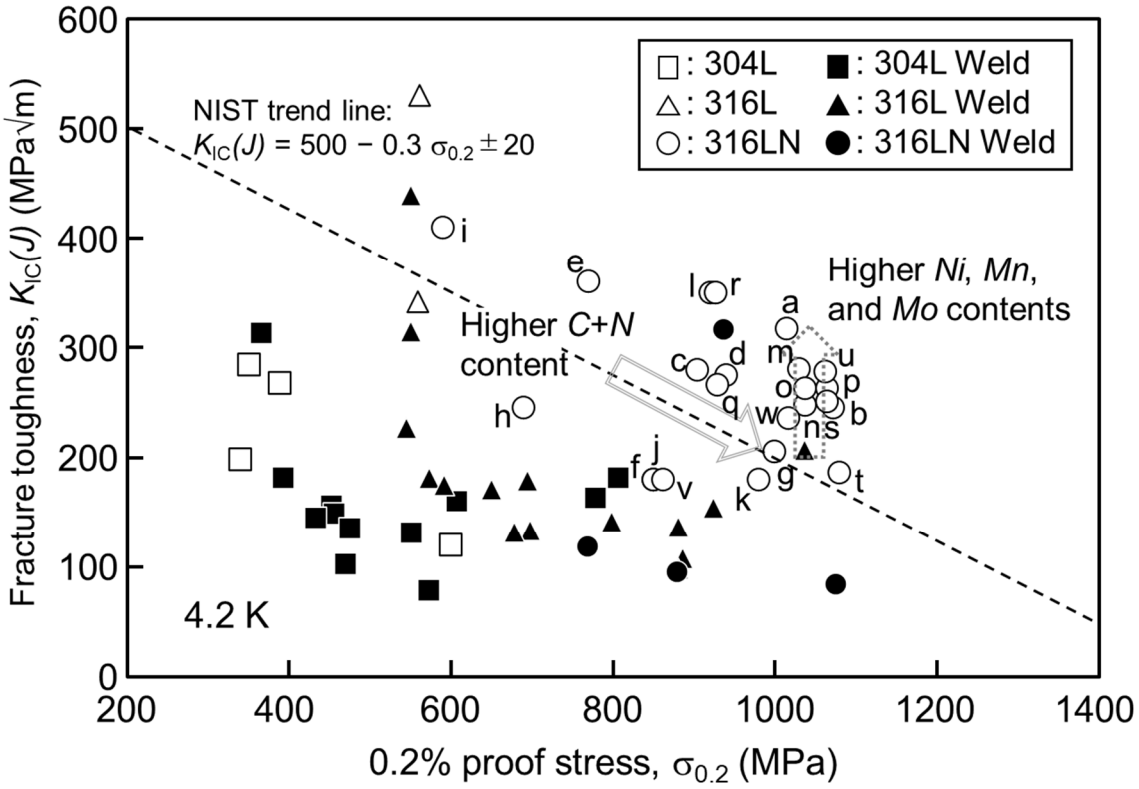

Figure 6. Relationship between $K_{IC}(J)$ and $\sigma_{0.2}$ of type 304L, 316L, and 316LN steels and their weldments at 4.2 K.

Figure 4 shows a plot of *C+N* content on the horizontal axis and $\sigma_{0.2}$ and σ_B on the vertical axis at 4.2 K. To check if there is a correlation between them and the *C+N* content, the approximate equations were added to figure 4 and the R^2 of each was evaluated. Figure 5 shows a plot of *C+N* content on the horizontal axis and $K_{IC}(J)$ on the vertical axis at 4.2 K.

At 4.2 K, $\sigma_{0.2}$ increases significantly with *C+N* content, especially the correlation between the $\sigma_{0.2}$ of the base material and *C+N* content is good as R^2 = 0.90. The increment of $\sigma_{0.2}$ of the weldments are larger than that of the base materials. On the other hand, the correlation between σ_B and *C+N* content is very low, with R^2 around 0.005. The weldments tend to have higher $\sigma_{0.2}$ and lower σ_B compared to the base materials due to the hardening by welding. $K_{IC}(J)$ at 4.2 K tends to decrease slightly with increasing *C+N* content, but they have a large variation. The $K_{IC}(J)$ for welding is low regardless of the steel type.

Figure 6 shows the relationship between $\sigma_{0.2}$ and $K_{IC}(J)$ with the NIST trend line. Type 316LN has increased the nitrogen content of 316L to achieve higher $\sigma_{0.2}$, but the fracture toughness decreases accordingly. A trade-off between the two was also observed in this report. However, many of the plots are on the high strength/high fracture toughness side of the NIST trend line because of the relatively high fracture toughness data included in this report. In addition, the weld plots are lower than the NIST trend line.

The fracture toughness of 316LN steel at 4.2 K depends on its phase stability to the α'-martensitic formation, which is characterized by the Md_{30} index. The Md_{30} is the temperature (K) at which 50% volume of the austenite matrix transforms to martensite under a true strain of 0.30 in tension for single phase austenitic steels [36]. The Md_{30} of the 316LN plates correlated well with their respective fracture toughness values, with a higher Md_{30} indicating lower fracture toughness [23]. Then, the fracture toughness at 4.2 K and martensitic transformation at the crack tip were evaluated for ITER grade 316LN thick plates with a relatively high $\sigma_{0.2}$ of approximately 1080 MPa [24]. The formation of shear bands at low strains was directly related to fracture toughness. The stacking fault energy represents the shear-band formation as well as slip deformation manner at the crack tip. An alloy design with a higher content

of Ni, Mn and Mo in its chemical composition would be favorable for 316LN steel to provide higher fracture toughness due to higher stacking fault energy. Data with high *Ni*-eq and *Cr*-eq, e.g., l, m, r, s, and u, shown in figure 2 appears high strength and high toughness. It is effective to improve the fracture toughness of 316LN steel with high *C+N* content to develop a material with a good balance between strength and toughness.

4. Conclusions

The tensile properties and fracture toughness of austenitic stainless steels, such as type 304L, 316L, and 316LN, and their weldments in the literature have been summarized and reviewed in relation to test temperature and *C+N* content. 316LN steel showed a good balance of high strength and high toughness at 4.2 K due to nitrogen solid solution strengthening. Especially for the base material, $\sigma_{0.2}$ increases significantly with *C+N* content. However, the alloy design with higher Ni, Mn, and Mo contents in the chemical composition range of 316LN would be desirable to improve fracture toughness as it decreases with increasing strength.

5. References

[1] Umezawa O 2021 *Mater. Performance and Characterization* **10(2)** 3–15 [10.1520/MPC20200138]
[2] Reed R P 1989 *JOM* **41(March)** 16–21 [10.1007/BF03220991]
[3] Simmons J W 1996 *Mater. Sci. Eng.* **A207** 159–169 [10.1016/0921-5093(95)09991-3]
[4] Sakurai T, Iguchi M and Nakahira M 2019 *Teion Kogaku* **54** 459–466 [10.2221/jcsj.54.459]
[5] Tobler R L and Reed R P 1980 Interstitial carbon and nitrogen effects on the tensile and fracture parameters of AISI 304 stainless steels *National Bureau of Standards International Report 80-1627* ed R P Reed (Boulder: NBS) pp 17–48 (https://nvlpubs.nist.gov/nistpubs/Legacy/IR/nbsir80-1627.pdf)
[6] Yoshida K *et al* 1983 *Austenitic Steels at Low Temperature* (New York: Plenum Press) pp 29–39 [10.1007/978-1-4613-3730-0_2]
[7] Nakajima H, Yoshida K and Shimamoto S 1990 *ISIJ Inter*. **30** 567–578 [10.2355/isijinternational.30.567]
[8] NEDO 1995 Result report of WE-NET sub-task 6 development the cryogenic material technology *NEDO-WE-NET-946*
[9] NEDO 1998 Result report of WE-NET sub-task 6 development the cryogenic material technology *NEDO-WE-NET-976*
[10] NIMS 2006 Data sheet on fracture toughness and high-cycle fatigue properties of forged 304L *Space Use Materials Strength Data Sheet No.7*
[11] Chan J W, Glazer J, Mei Z and Morris Jr. J W 1990 *Adv. Cryo. Eng*. **36B** 1299–1306
[12] Fukushima E, Kobatake S, Tanaka M and Ogiwara H 1987 *11th Conference on Magnet Technology* 127–130
[13] Murase S *et al* 1993 *Fusion Eng. Design* **20** 451–454 [10.1016/0920-3796(93)90078-V]
[14] Nishimura A *et al* 1997 *Adv. Cryo. Eng. Maters.* **42A** 315–322
[15] Yuri T, Nagai K and Ishikawa K 1990 *Teion Kogaku* **25** 35–41 [10.2221/jcsj.25.35]
[16] NEDO 2000 Result report of WE-NET Phase II R&D task 10 development the cryogenic material *NEDO-WE-NET-9910*
[17] Simon N J and Reed R P 1988 *Adv. Cryo. Eng. Maters*. **34** 165–172
[18] Chan J W, Chu D, Tseng C and Morris, Jr. J W 1994 *Adv. Cryo. Eng. Maters*. **40** 1215–1221 [10.1007/978-1-4757-9053-5_154]
[19] Ogata T *et al* 1990 *Adv. Cryo. Eng*. **36B** 1053–1060
[20] Ogata T *et al* 1994 *Adv. Cryo. Eng.* **40A** 1191–1198 [10.1007/978-1-4757-9053-5_151]
[21] Ogata T *et al* 1992 *Adv. Cryo. Eng*. **38A** 69–76 [10.1007/978-1-4757-9050-4_9]
[22] Nyilas A and Yanagi H 1989 *Cryogenics* **29** 191–195 [10.1016/0011-2275(89)90082-9]
[23] Sakurai T *et al* 2017 *Teion Kogaku* **52** 260–267 [10.2221/jcsj.52.260]
[24] Sakurai T and Umezawa O 2023 *Mater. Sci. Eng. A* **862** 144122 [10.1016/j.msea.2022.144122]
[25] Sa J W *et al* 2006 *Proc. 21st IEEE/NPS Symp. on fusion Eng.*

(https://www.kns.org/files/pre_paper/18/434%EC%82%AC%EC%A0%95%EC%9A%B0.pdf)
[26] Nyilas A, Portone A and Kiesel H 2002 *Adv. Cryo. Eng*. **48** 123–130 [10.1063/1.1472534]
[27] NEDO 1997 Result report of WE-NET sub-task 6 development the cryogenic material technology *NEDO-WE-NET-966*
[28] NEDO 1999 Result report of WE-NET sub-task 6 development the cryogenic material technology *NEDO-WE-NET-986*
[29] NEDO 2001 Result report of WE-NET Phase II R&D task 10 development the cryogenic material *NEDO-WE-NET-0010*
[30] Whipple T A and Kotecki D J 1981 Material studies for magnetic fusion energy applications at low temperature - IV *National Bureau of Standards International Report 81–1645* ed R P Reed and N J Simon (Boulder: NBS) pp 303–321 (https://www.govinfo.gov/content/pkg/GOVPUB-C13-cc544300a6d8dc7c4d297097ae4aea97/pdf/GOVPUB-C13-cc544300a6d8dc7c4d297097ae4aea97.pdf)
[31] Read D T, McHenry H I, Steinmeyer P A and Thomas, Jr. R D 1980 *Welding J*. **59** 104s–113s (https://app.aws.org/wj/supplement/WJ_1980_04_s104.pdf)
[32] NEDO 2002 Result report of WE-NET Phase II R&D task 10 development the cryogenic material *NEDO-WE-NET-0110*
[33] McHenry H I, Read D T and Steinmeyer P A 1979 Material studies for magnetic fusion energy applications at low temperature - II *National Bureau of Standards International Report 79–1609* ed F R Fickett and R P Reed (Boulder: NBS) pp 299–312 (https://nvlpubs.nist.gov/nistpubs/Legacy/IR/nbsir79-1609.pdf)
[34] DeLong W T 1974 *Welding J.* **53** 273s–286s (https://app.aws.org/wj/supplement/WJ_1974_07_s273.pdf)
[35] Kujanpää V, Suutala N, Takao T and Moisio T 1979 *Welding Research Int.* **9** 55–76
[36] Angel T 1954 *J. Iron Steel Inst.* **177** 165–174

Acknowledgments
Authors would like to thank colleagues in National Institutes for Quantum Science and Technology, and National Institute for Materials Science for their supports on this work.